



Assessment of the Characteristics of Different Kinds of MS Lesions Using Multi-Parametric MRI

Asieh Fatemidokht ¹, Mohammad Hossein Harirchian ^{2,3}, Elham Faghihzadeh ⁴, Abbas Tafakhori ^{2,3} and Mohammad Ali Oghabian ^{1,5,*}

¹Medical Physics and Biomedical Engineering Department, Tehran University of Medical Sciences, Tehran, Iran

²Iranian Center of Neurological Research, Neuroscience Institute, Imam Khomeini Hospital, Tehran University of Medical Sciences, Tehran, Iran

³Department of Neurology, Imam Khomeini Hospital, Tehran University of Medical Sciences, Tehran, Iran

⁴Department of Biostatistics, Faculty of Allied Medical Sciences, Shahid Beheshti University of Medical Sciences, Tehran, Iran

⁵Neuroimaging and Analysis Group (NIAG), Tehran University of Medical Sciences, Tehran, Iran

*Corresponding author: Medical Physics and Biomedical Engineering Department, Tehran University of Medical Sciences, Tehran, Iran. Tel: +98-2166907518-9, Fax: +98-2166581533, Email: oghabian@sina.tums.ac.ir

Received 2020 March 26; Revised 2020 July 06; Accepted 2020 July 12.

Abstract

Background: Studying different pathological aspects of lesions in multiple sclerosis (MS) patients could be useful to modify the diagnosis and treatment of this neurological disorder. Magnetic resonance imaging (MRI) modalities have the potential to investigate variations in brain tissue because of inflammatory and neurodegenerative processes in various types of MS-related lesions.

Objectives: This study was done to investigate the quantitative changes in MRI-based parameters, like perfusion and magnetization transfer ratio (MTR) of different types of brain lesions, to demonstrate the ability of MRI to detect structural and pathological differences in MS lesions.

Methods: Quantitative MRI modalities were performed on 18 patients with five different kinds of lesions (T1 holes, acute and chronic white matter (WM), and acute and chronic gray matter (GM) lesions) using a 3 T MRI scanner. The following protocols were used to characterize the pathology of lesions: (I) fluid-attenuated inversion recovery (FLAIR); (II) pre- and post-contrast T1-weighted; (III) dynamic contrast-enhanced (DCE); and (IV) MTR imaging. Quantitative comparison of Ktrans, cerebral blood volume (CBV), cerebral blood flow (CBF), and MTR was done to find the best parameter to distinguish different lesions. Finally, a multivariate classifier was applied to introduce the best parameter to indicate differences in lesions.

Results: Five lesions were characterized by perfusion and MTR parameters. The pathological changes were measured, including: (I) the highest value of parameters in both acute WM and GM lesions; (II) the lowest value of four parameters in both chronic WM and GM lesions; (III) MTR had the highest rank among parameters using the classifier.

Conclusions: The degree of pathological alterations due to inflammatory and neurodegenerative processes in MS-related lesions was indicated through the used parameters in different kinds of lesions. Inflammation was the dominant process in acute lesions, while neurodegeneration and tissue loss were observed mostly in chronic lesions. Both inflammation and neurodegeneration were detected in T1 holes. Perfusion parameters and MTR were reasonable parameters to describe differences in brain lesions. Thus, it could be confirmed that magnetization transfer imaging (MTI) and DCE-MRI are high-sensitivity methods to detect microstructural changes in the brain and subtle changes in the blood-brain-barrier. Classification of the parameters indicated that MTR was the best biomarker than others to show variations in lesions pathology.

Keywords: Multi-Parametric MRI, DCE-MRI, MTI, Multiple Sclerosis

1. Background

Multiple sclerosis (MS) is the most common immune-mediated inflammatory demyelinating disease of the central nervous system (CNS) with a prevalence of 30 per 100,000 (with a range of 5 - 80) worldwide (1). Magnetic resonance imaging (MRI) is an important diagnostic tool for MS because it produces clear images of pathological changes in lesions in the brain and spinal cord of MS pa-

tients. Thus, it could be useful to monitor the statuses of disease and how the patient responds to treatment (2). MRI has improved the diagnostic work-up in monitoring statuses of MS patients, but inappropriate conventional techniques could effect on detection of different kinds of lesions; for example, some MRI artifacts in T2-fluid-attenuated inversion recovery (FLAIR) images could be considered as brain lesions or patient's small move-

ment changes the detection of the lesions. Also, subtle changes at the onset of brain tissue damage have not been seen in conventional images. Therefore, appropriate protocols, like dynamic contrast-enhanced (DCE)-MRI, can detect dysfunction of blood-brain-barrier (BBB), which occurs in the early stages of the inflammatory cascade process and are beneficial in the early stages of newly forming lesions that are not seen in conventional protocols, like T1 or T2-FLAIR. Improvements in MRI techniques and the use of appropriate MRI protocols based on variation in the brain during MS can be promising for a better definition of the typical parameters of MS lesions (3).

MS-related lesions can be appeared on MRI images as either bright or dark spots, depending on the type of MRI protocols used. In T2-weighted MRI protocol is applied commonly to quantify the lesion load and T1-weighted to differentiate edema, blood-brain barrier (BBB) breakdown by contrast enhancement, and irreversible brain tissue damage (black holes) (4). Pathologically, in different kinds of MS lesions, active enhanced lesions hallmark damages BBB, which leads to the infiltration of the inflammatory cells into the CNS. Thus, the inflammatory demyelination and vasogenic edema present in early MS lesions and active lesions. Chronic lesions are more frequent in progressive MS patients and are characterized by a slowly expanding rim of activated brain immune cells (microglia) (5). Perivascular inflammatory infiltrates are often encountered in chronic lesions. As the lesions progress from acute active to chronic lesions, edema resolves, inflammation decreases, and brain immune cells gradually disappear. Accordingly, axonal damage and loss are also observed in chronic lesions. T1-black holes may represent either area of edema or axonal loss and severe tissue destruction, which are a marker of neuronal loss and neurodegeneration in brain tissue and measure disease activity in progressive MS patients (6). T1 black holes result from an expansion of the extracellular space due to an increase in water content or deterioration of structural components (7). Conventional MRI (CMRI) is a useful prognostic tool to obtain valuable information about the number, location, and inflammatory activity of MS-related lesions, but it provides limited sensitivity to pathology alteration in the cortex and principle of focal damage. Thus, the advanced modality of MRI could give us an insight into focal damage and pathology of different kinds of lesions, such as axonal and myelin damage (8-12). DCE-MRI gives information about subtle BBB alteration in lesions, which help us to quantify immunity cells infiltration and activity of lesions. Perfusion parameters, like cerebral blood flow and cerebral blood volume, are proper markers to investigate the amount of delivered blood to different kinds of MS lesions and hemodynamic changes in the brain and could be a clue to the pres-

ence of inflammation in different kinds of MS lesions (13). Also, magnetization transfer imaging is a good modality to quantify vasogenic edema and abnormality in water content or damaged structure of brain tissue, which are observed in chronic MS lesions (14). Therefore, a combination of imaging modalities could provide quantitative information to distinguish active, chronic, and black hole lesions (15).

2. Objectives

In this study, multi-parametric quantitative MRI modalities were used to investigate the amount of inflammation-related alterations in different kinds of MS lesions to obtain the following objectives: (A) introduction of a hallmark biomarker to differentiate between the types of lesions; (B) introduction of a multi-parametric MRI protocol to use in clinical MRI to detect subtle alterations caused by inflammation in active and chronic lesions.

3. Methods

3.1. Subjects

Images of 18 patients with a clinical diagnosis of relapse-remitted multiple sclerosis (RRMS) using MacDonald Criteria (16), who were admitted at MS Clinic of the Research Institute of Neurology in Imam Hospital in Tehran, Iran, were obtained with conventional and DCE-MRI and magnetization transfer imaging protocols. Table 1 shows the details of the patient's demographic descriptions. MRI, according to a standard clinical MS protocol with the addition of multi-parametric MRI before and after administration of a gadolinium-based contrast agent, was performed. The local institutional review board approved the study, and written informed consent was obtained from all patients.

Table 1. Demographic Characteristics and Clinical Description of the Disease Stage of Multiple Sclerosis (MS) Patients

| | MS Patients | |
|---|-------------|---------|
| | Female | Male |
| Number of patients | 6 | 12 |
| Median age, y | 43 | 31 |
| Age range, y | 31 - 50 | 27 - 62 |
| Disease duration, y | 2 - 10 | 5 - 15 |
| EDSS | 0 - 4 | 1 - 5 |
| The last replace before inclusion, week | 2 - 6 | 2 - 6 |

Abbreviation: EDSS, expanded disability status state.

3.2. MRI imaging Acquisition

Images were acquired on a 3 Tesla MRI scanner (DISCOVERY MR750w: GE Healthcare, Chicago, Illinois, United States) using a 24-channel phased-array head coil. The main acquisition parameters of the sequence are presented in Table 2.

Table 2. Main Acquisition Parameters of the Magnetic Resonance Imaging (MRI) Sequences Used for Imaging

| Sequence | Acquisition Parameters | Values |
|---|------------------------|---------------------------|
| DCE sequence | | AX 3D-SPGR |
| | TR | 3.34 ms |
| | TE | 1.28 ms |
| | FOV | 300 × 300 mm ² |
| | Slice number | 900 |
| | Thickness | 5 |
| MT sequence | | AX 3D-SPGR |
| | TR | 28 ms |
| | TE | 5 ms |
| | FOV | 240 × 240 mm ² |
| | Slice number | 64 |
| | Thickness | 2 |
| Pre- and post-contrast T1-weighted sequence | | AX 2D-SE |
| | TR | 6000 ms |
| | TE | 11 ms |
| | FOV | 230 × 230 mm ² |
| | Slice number | 23 |
| | Thickness | 5.5 |
| FLAIR | | AX, COR 2D-FSE |
| | TR | 8000 |
| | TE | 119.88 |
| | FOV | 230 × 230 mm ² |
| | Thickness | 5.5 |

Abbreviations: 3D-SPGR, 3-dimensional spoiled gradient-echo; ETL, echo time length; FOV, field of view; FSE, fast spin-echo; MT, magnetization transfer; SE, spin echo; TE, echo time; TR, repetition time.

3.2.1. Image Analysis

To assure that the injection rates and patients' cardiovascular states do not affect the kinetic parameters, the arterial input function (AIF) was incorporated into the two-compartment model. Here, the AIF corrected the kinetic analysis by measuring the signal from the regions of interest (ROI) in the middle cerebral artery on T1-weighted

images and adjusting the results accordingly. Other ROIs located in T1 hole, acute white matter (WM), chronic WM, acute gray matter (GM), and chronic GM (Table 2 and Figure 1) indicate different lesions in T2-FLAIR and post-contrast T1-weighted images. ROIs were outlined manually by an experienced radiologist. First, in post-contrast T1 ROI was manually placed on the enhancement of active lesions. Then, ROIs were masked and placed on T2-FLAIR images in MRI-CRO (Nottingham, UK) because FLAIR images had the best contrast to determine MS lesions. In chronic lesions without any gadolinium (Gd)-enhancement, ROIs manually were drawn on selected lesions in T2-FLAIR images. Finally, ROIs were placed on perfusion-weighted imaging (PWI) images. The magnitude of enhancement varied across the lesion. Acute active lesions in both WM and GM were determined by comparing pre- and post-contrast T1-weighted images, and all of the T1-weighted images were compared with T2-FLAIR because of the high detectability of different kinds of lesions in this sequence. Recognized chronic lesions from T2-FLAIR images were compared with post-contrast T1-weighted images to ensure that there was no Gd uptake. Also, obtained images from 3D-SPGR protocol in magnetization transfer imaging (MTI) could be beneficial in cortical GM lesions. The supervised assistant neurologist confirmed all detected lesions. The obtained ROIs of perfusion-weighted images were then analyzed using the DCE Tool plug-in (version 2.0SP1) within ClearCanvas (Toronto, Ontario, Canada) framework. The DCE Tool provides options to model contrast uptake within an ROI using the modified Toft's model (17). The DCE Tool computed these metrics for each ROI. The most important physiologic parameter of the tissue is Ktrans, which demonstrates a combination of both tissue perfusion and permeability. Also, in-house developed MATLAB code was used to obtain cerebral blood volume (CBV) and cerebral blood flow (CBF) of the mentioned lesions measured by perfusion parameters in the DCE-MRI sequence. In MT and non-MT data, ROIs of each kind of lesions were drawn manually in MRI-CRO software, and signal intensity in both MT and non-MT images were measured. The MTR parameter was measured using the following Equation 1:

$$MRT = \frac{M_s - M_0}{M_0} \tag{1}$$

Where M₀ is the value of the signal in non-MT images and M_s is the value of the signal in MT images.

3.3. Statistical Analysis

Each of the four parameters was assessed (both mean and SD of MTR, Ktrans, CBV, and CBF) in different kinds of lesions (T1 holes, acute and chronic WM, and acute and chronic GM). A multi-parametric test (ANOVA) was used to

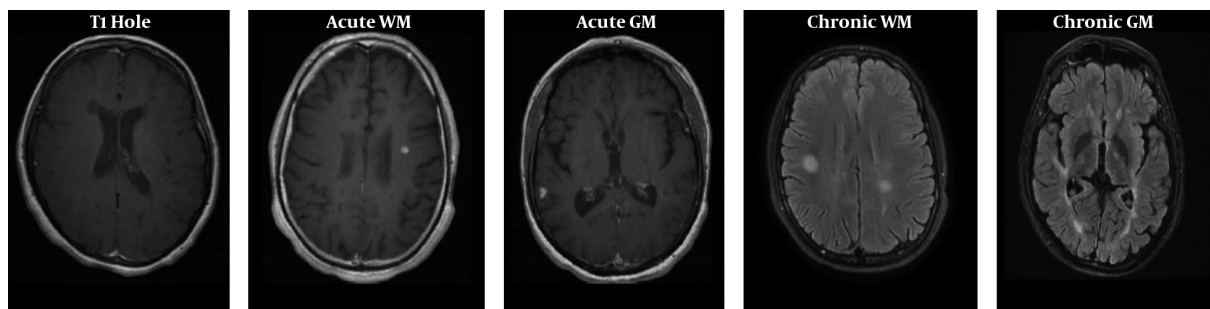


Figure 1. Illustration of the lesion appearance of T1 hole in T1-weighted images, acute gadolinium-enhancing white matter (WM) and grey matter (GM) lesions in T1-weighted images, and chronic WM and GM lesions in T2-FLAIR images, respectively.

detect significant differences using SPSS version 21.0 software (SPSS Inc., Chicago, IL, USA). Finally, a multivariate analysis using support vector machines (SVMs) was performed using Weka3 (University of Waikato). This classifier showed the best parameter to show differences between lesions.

4. Results

Five groups of lesions in T2-FLAIR and post-contrast scans are displayed in [Figure 1](#). Also, the Ktrans and MTR maps in marked lesions are represented in [Figure 2](#).

Analysis of four parameters of Ktrans, CBF, CBV, and MTR in five groups of lesions showed significant differences between each parameter in different kinds of MS lesions, which are represented in [Table 3](#). The Ktrans mean value of acute GM lesions was the highest value among the five groups of lesions. Except for CBV, other parameters showed similar results to Ktrans. As shown in [Table 3](#), the p-values of all measured parameters obtained by the ANOVA were less than 0.05, thus, these parameters had significant differences. The values of the parameters of Ktrans, CBV, CBF, and MTR are displayed in [Figure 3](#), respectively.

To investigate differences between two groups of acute and chronic lesions in WM and GM lesions, a t-test was applied, and the results for WM acute and chronic lesions showed significant differences between Ktrans, CBV, and CBF ($P < 0.05$) ([Table 4](#)). Regarding acute and chronic lesions in GM, only CBF had a significant difference ($P < 0.05$) between the two groups ([Table 5](#)).

The SVM was used to indicate the best parameter between four parameters in different types of lesions, which measured the mean value of parameters to introduce appropriate biomarkers to demonstrate different characteristics of the lesions. The results indicated the feature weights, respectively, as follows: MTR, CBV, CBF, and Ktrans ([Table 6](#)). According to the measured SVM classifier rank

Table 3. The Analysis of Variance (ANOVA) Results of the Four Parameters (Ktrans, CBV, CBF, and MTR) in Five Kinds of T1 Hole, Acute WM, Chronic WM, acute GM, and Chronic GM^a

| | Numbers | Values | ANOVA; P Value |
|---------------|---------|---------------|----------------|
| KTRANS | | | < 0.001 |
| T1 hole | 20 | 0.26 ± 0.22 | |
| Acute WM | 20 | 0.51 ± 0.34 | |
| Chronic WM | 80 | 0.14 ± 0.12 | |
| Acute GM | 6 | 0.69 ± 0.58 | |
| Chronic GM | 24 | 0.13 ± 0.13 | |
| CBV | | | 0.048 |
| T1 hole | 20 | 1.37 ± 1.05 | |
| Acute WM | 20 | 1.98 ± 0.98 | |
| Chronic WM | 80 | 1.25 ± 0.82 | |
| Acute GM | 6 | 1.96 ± 0.94 | |
| Chronic GM | 24 | 1.11 ± 1.04 | |
| CBF | | | < 0.001 |
| T1 hole | 20 | 25.75 ± 6.27 | |
| Acute WM | 20 | 29.52 ± 12.14 | |
| Chronic WM | 80 | 21.45 ± 6.71 | |
| Acute GM | 6 | 32.49 ± 12.67 | |
| Chronic GM | 24 | 17.53 ± 5.37 | |
| MTR | | | < 0.001 |
| T1 hole | 20 | 0.43 ± 0.07 | |
| Acute WM | 20 | 0.62 ± 0.04 | |
| Chronic WM | 80 | 0.63 ± 0.03 | |
| Acute GM | 6 | 0.59 ± 0.01 | |
| Chronic GM | 24 | 0.55 ± 0.09 | |

^aValues are expressed as mean ± SD.

weights, MTR was the best biomarker to distinguish between five kinds of lesions.

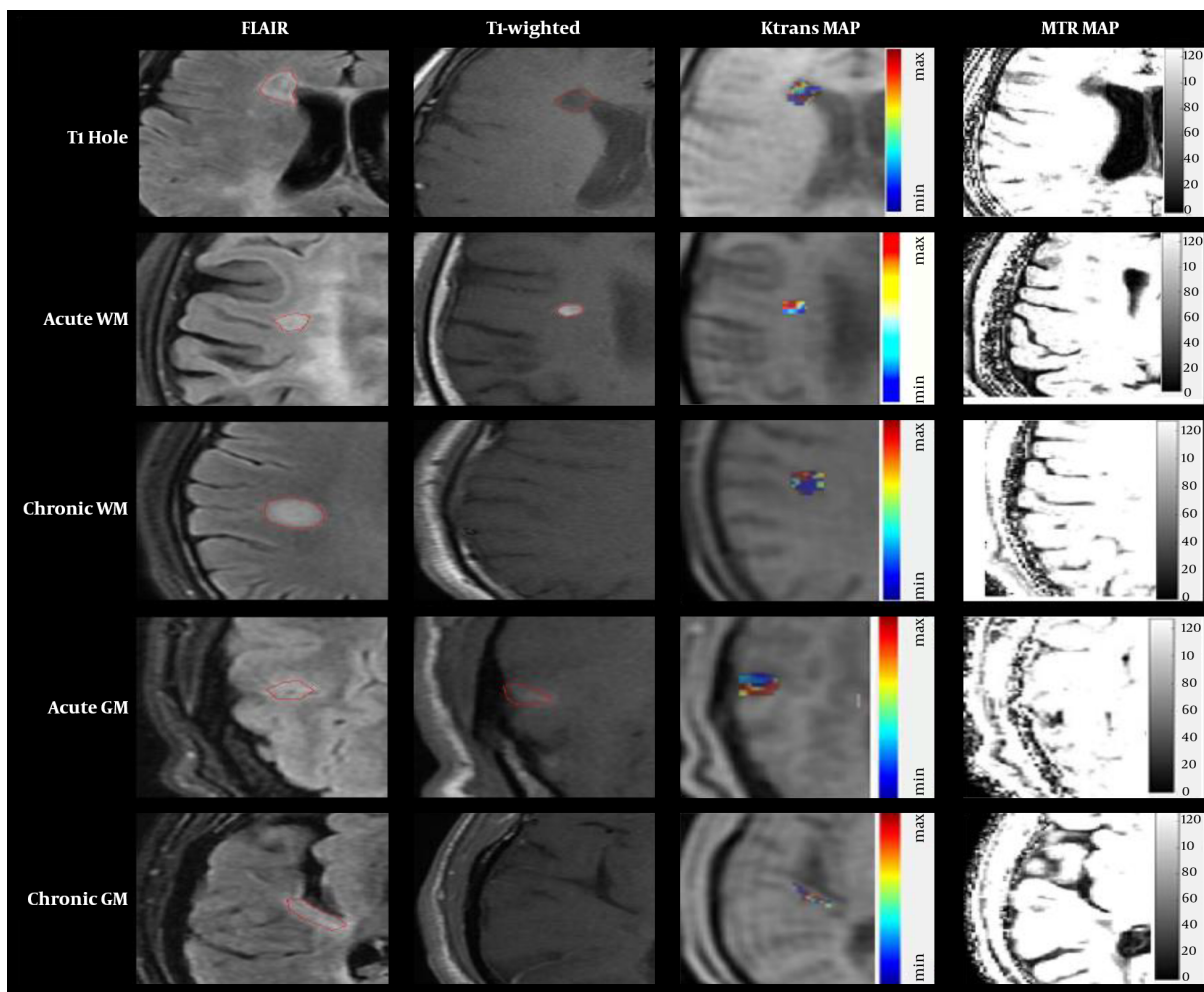


Figure 2. Left columns, Lesions in two MRI-modalities of T2-FLAIR and T1-weighted images; right columns, Ktrans and MTR map with their color bar in the FLAIR and T1-weighted images. The lesions are displayed by red markers.

5. Discussion

The aim of this study was to assess whether non-conventional multi-parametric quantitative MRI can be used to detect the pathological change in various types of MS-related lesions changes, like subtle BBB dysregulation and microstructural variations that cannot be revealed by conventional protocols. Therefore, the development of a proper method to differentiate between different kinds of lesions that have not yet been investigated is beneficial to demonstrate pathological changes during different stages of MS. In this study, four quantitative parameters were investigated in different types of lesions in MS patients. Also, this study assessed alterations based on different aspects of inflammation in various MS-related lesions reviewed earlier by researchers. Previous studies have proved that

MS acute lesions massively were contributed to perivascular and parenchymal inflammatory infiltrate and also have demonstrated that inflammation was the reason for demyelination and axonal degeneration, which can be observed in chronic and black holes lesions (5, 18). According to the remarkable ability of MRI modalities to detect subtle changes in the brain, DCE-MRI had the potential to detect alteration caused by inflammation. Applied methods in this research could reveal alterations that happened during inflammatory processes in the brain (19), and multi-parametric MRI could show inflammatory-related changes by an observed abnormality in T1, T2, and T2* relaxation time and MT ratio (20). Dynamic imaging of the hemodynamic changes during inflammatory diseases, like MS, has shown abnormality in cerebral permeability, which can indicate dysfunction BBB in MS brains compared with

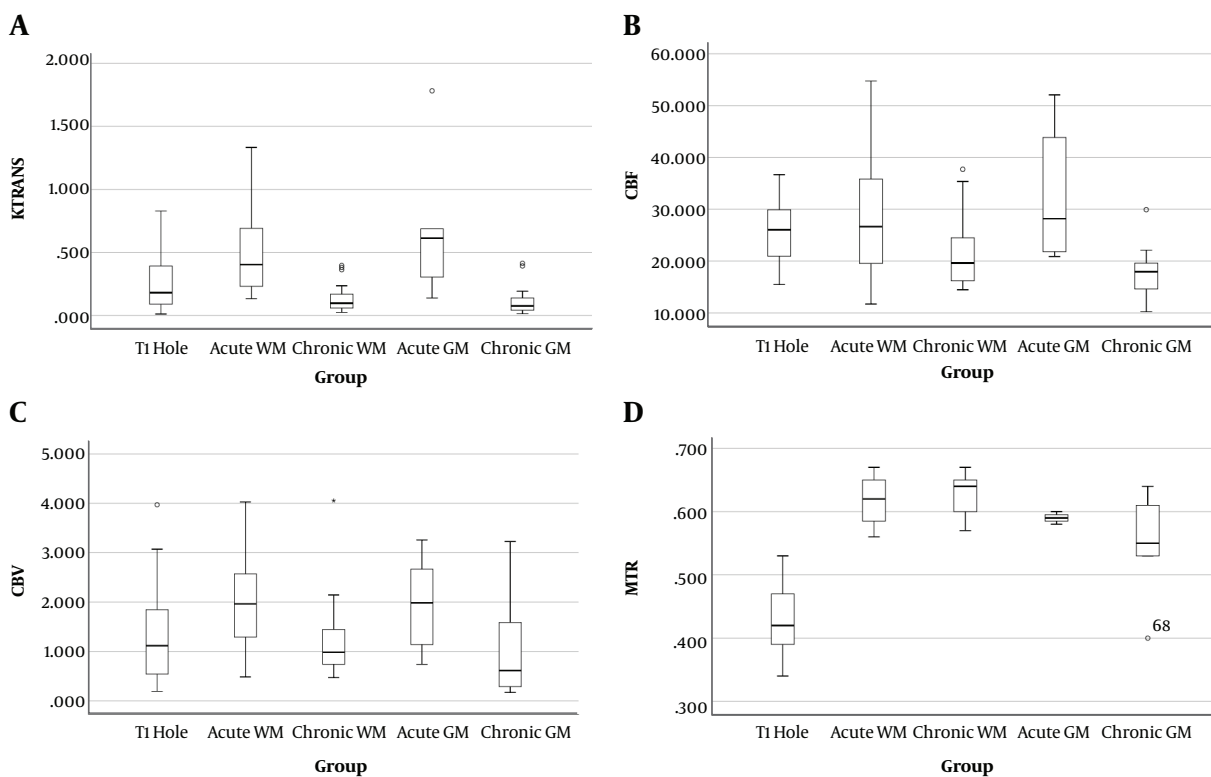


Figure 3. A, Comparison of the Ktrans; B, cerebral blood flow (CBF); C, cerebral blood volume (CBV); D, and magnetization transfer ratio (MTR) parameters in various lesions. Box plots represent the median value (50th percentile) and the range of density of the lesions. Outliers marked with a circle are mean values of each parameter in certain lesions.

Table 4. The *t*-test Results Comparing Four Parameters of Ktans, CBV, CBF and MTR in Acute and Chronic WM Lesions^a

| Group | Values | P Value |
|---------------|---------------|---------|
| KTRANS | | < 0.001 |
| Acute WM | 0.51 ± 0.34 | |
| Chronic WM | 0.14 ± 0.12 | |
| CBV | | 0.014 |
| Acute WM | 1.98 ± 0.98 | |
| Chronic WM | 1.25 ± 0.82 | |
| CBF | | 0.013 |
| Acute WM | 29.52 ± 12.14 | |
| Chronic WM | 21.45 ± 6.71 | |
| MTR | | 0.577 |
| Acute WM | 0.62 ± 0.04 | |
| Chronic WM | 0.63 ± 0.03 | |

^aValues are expressed as mean ± SD.

Table 5. The *t*-test Results Comparing Four Parameters of Ktans, CBV, CBF, and MTR in Acute and Chronic GM Lesions^a

| Group | Values | P Value |
|---------------|---------------|---------|
| KTRANS | | 0.063 |
| Acute GM | 0.69 ± 0.58 | |
| Chronic GM | 0.13 ± 0.13 | |
| CBV | | 0.107 |
| Acute GM | 1.96 ± 0.94 | |
| Chronic GM | 1.11 ± 1.04 | |
| CBF | | 0.033 |
| Acute GM | 32.49 ± 12.67 | |
| Chronic GM | 17.53 ± 5.37 | |
| MTR | | 0.383 |
| Acute GM | 0.59 ± 0.01 | |
| Chronic GM | 0.55 ± 0.09 | |

^aValues are expressed as mean ± SD.

Table 6. The Results of the Comparison of Lesions Using SVM Classifier to Determine the Best Parameter to Distinguish Different Kinds of Lesions

| Parameter Rank | Parameter | SVM Weight |
|----------------|-----------|------------|
| 1 | MTR | 1.074 |
| 2 | CBV | 0.527 |
| 3 | CBF | 0.326 |
| 4 | KTRANS | 0.092 |

normal volunteers (21). In agreement with the results of other studies, measured perfusion parameters, like Ktrans, CBV, and CBF in various lesions had significant differences between chronic and active lesions, which indicates that their values changed differentially in all lesions and could be a proper biomarker to detect the number of perfusion changes in MS-related lesions. A high value of Ktrans, CBV, and CBF has been observed in acute lesions related to structural changes during inflammation. The low value of parameters in chronic lesions, including black holes, has been shown due to neurodegeneration in these lesions, which is associated with neuronal and axonal loss (22). Until now, there is no study on all lesions in MS brains; however, several studies have reported a reduction in CBV and CBF in MS lesions, which had a significant difference between normal white and GM (23). Cortical GM damage is now widely recognized in MS. The standard MRI does not reliably detect cortical GM lesions. Therefore, advanced protocols, like 3D-spoiled gradient recalled echo that is used in MT imaging, could reliably and quantitatively assess cortical GM damages, like active or chronic lesions in MS patients, as our results showed (24).

Measurements of perfusion characteristics in MS lesions compared with the normal-appearing WM have been shown that BBB interruption has an important role in enhancement and uptake of Gd-based contrast agents and could demonstrate inflammatory activation in acute MS lesions. Also, DCE-MRI has a high sensitivity to reveal dysfunction of BBB earlier than routine protocols, such as post-contrast T1-weighted images (25). Evaluations of the black holes have confirmed the results of other investigators, indicating the presence of edema and axonal loss in T1 holes with a higher value of quantitative parameters than chronic lesions associated with axonal loss and neuronal degeneration (6, 22, 26). Magnetization transfer imaging investigations on MS patients have been recently considered, and this modality could show microstructural changes during the formation of MS lesions. The presence of inflammation and vasogenic edema in MS-related lesions can cause an increase in the water content of brain tissue (27). Measurements of the microstructure of lesions in long-term evolution in normal-appearing WM and MS le-

sions have shown a significant decrease in this parameter that is contributed to an abnormality in MS lesions, which is consistent with our results. Non-conventional MRI investigations on MS lesions have shown the relevance between MTR and myelin content of lesions, which has been shown by a comparison between histopathological analysis and MTI. They have shown a greater pathologic specificity compared with standard protocols that were confirmed by our results (28-30). Our ANOVA results showed that MTR also changed significantly in different kinds of lesions, which was related to the pathology of the lesions (5, 22). A short-lived inflammatory process has been observed in acute MS lesions. The pathology of lesions has demonstrated that the content of myelin in black holes had the lowest value in MTR because of the persistence effect of neuronal and axonal loss. Also, destroyed myelin in chronic lesions is more than active lesions because of the presence of edema and microglia activation in acute lesions. Accordingly, measurements have shown that the MTR had a lower value in chronic lesions (31, 32).

SVM classifier analysis was performed to define the best parameter, which showed the best rank weights between measured parameters in all kinds of lesions. Due to the differences in measured parameters, MTR was indicated as the best parameter to show the difference between normal WM and MS lesions (20). Also, this research introduced MTR as the best biomarker to indicate significant differences between different types of lesions, and MTR was an appropriate parameter to differentiate between various types of MS-related lesions.

5.1. Conclusions

Recently, impressive progress has been made in the investigation of several aspects of advanced MRI techniques, which has provided a detailed and new outlook into the pathological-related alterations in brain tissue during MS. Histopathological and imaging methods have indicated that inflammatory and neurodegenerative phenomena have important roles in MS lesions pathology. This study assessed appropriate parameters, like MTR and perfusion parameters, to describe pathology alterations in lesions. MTR changes may reveal the formation of acute active MS lesions several months before observation by conventional protocols. Thus, MTI is a modality that could reveal processes involved in the formation of active lesions. Also, DCE-MRI with high sensitivity to subtle changes in BBB could detect early changes in the formation of active lesions. Thus, the proposed protocols could be useful for early detection of newly forming lesions before T1 or T2-FLAIR images as well as for earlier diagnosis of the disease stage and save the time to begin treatment. This research tried to evaluate quantitative MRI methods to distinguish

different kinds of MS-related lesions, and our results introduced MRI parameters to indicate structural and pathological differences in the lesions, which were related to the inflammatory and neurodegenerative process. Finally, one of the measured parameters was introduced as the best parameter to indicate differences in lesions associated with water and myelin content of brain tissue.

In summary, multi-parametric MRI could assess and determine changes in lesions that cannot be provided by conventional and clinical routine MRI. Thus, the mentioned modality can help to reveal subtle changes in MS lesions with different microstructural and pathological changes related to inflammation.

Acknowledgments

The authors thank the Multiple Sclerosis Clinic of Imam Khomeini Hospital, Tehran, Iran, to concert the subjects and Imam Khomeini Medical Imaging Center, Tehran, Iran, for imaging data acquisition.

Footnotes

Authors' Contribution: None declared by author.

Conflict of Interests: No conflict of interests was declared.

Ethical Approval: The ethics code was IR.TUMS.MEDICINE.REC.1396.2662.

Funding/Support: This study was funded by the Tehran University of Medical Sciences (no.: 95-04-30-33430).

Informed Consent: Informed written consent was obtained from all patients for participating in this study and using their imaging data.

References

1. Daltrozzi T, Hapfelmeier A, Donnachie E, Schneider A, Hemmer B. A systematic assessment of prevalence, incidence and regional distribution of multiple sclerosis in Bavaria From 2006 to 2015. *Front Neurol*. 2018;**9**:871. doi: [10.3389/fneur.2018.00871](https://doi.org/10.3389/fneur.2018.00871). [PubMed: 30425676]. [PubMed Central: [PMC6218432](https://pubmed.ncbi.nlm.nih.gov/PMC6218432/)].
2. Traboulsee AL, Li DK. The role of MRI in the diagnosis of multiple sclerosis. *Adv Neurol*. 2006;**98**:125-46. [PubMed: 16400831].
3. Filippi M, Rocca MA, Barkhof F, Bruck W, Chen JT, Comi G, et al. Association between pathological and MRI findings in multiple sclerosis. *Lancet Neurol*. 2012;**11**(4):349-60. doi: [10.1016/S1474-4422\(12\)70003-0](https://doi.org/10.1016/S1474-4422(12)70003-0). [PubMed: 22441196].
4. Filippi M, Preziosa P, Banwell BL, Barkhof F, Ciccarelli O, De Stefano N, et al. Assessment of lesions on magnetic resonance imaging in multiple sclerosis: Practical guidelines. *Brain*. 2019;**142**(7):1858-75. doi: [10.1093/brain/awz144](https://doi.org/10.1093/brain/awz144). [PubMed: 31209474]. [PubMed Central: [PMC6598631](https://pubmed.ncbi.nlm.nih.gov/PMC6598631/)].
5. Popescu BF, Lucchinetti CF. Pathology of demyelinating diseases. *Annu Rev Pathol*. 2012;**7**:185-217. doi: [10.1146/annurev-pathol-011811-132443](https://doi.org/10.1146/annurev-pathol-011811-132443). [PubMed: 22313379].

6. Bagnato F, Jeffries N, Richert ND, Stone RD, Ohayon JM, McFarland HF, et al. Evolution of T1 black holes in patients with multiple sclerosis imaged monthly for 4 years. *Brain*. 2003;**126**(Pt 8):1782-9. doi: [10.1093/brain/awg182](https://doi.org/10.1093/brain/awg182). [PubMed: 12821527].
7. Brex PA, Molyneux PD, Smiddy P, Barkhof F, Filippi M, Youssry TA, et al. The effect of IFNbeta-1b on the evolution of enhancing lesions in secondary progressive MS. *Neurology*. 2001;**57**(12):2185-90. doi: [10.1212/wnl.57.12.2185](https://doi.org/10.1212/wnl.57.12.2185). [PubMed: 11756595].
8. Lassmann H. The pathologic substrate of magnetic resonance alterations in multiple sclerosis. *Neuroimaging Clin N Am*. 2008;**18**(4):563-76. ix. doi: [10.1016/j.nic.2008.06.005](https://doi.org/10.1016/j.nic.2008.06.005). [PubMed: 19068402].
9. Matthews PM, Piore E, Narayanan S, De Stefano N, Fu L, Francis G, et al. Assessment of lesion pathology in multiple sclerosis using quantitative MRI morphometry and magnetic resonance spectroscopy. *Brain*. 1996;**119** (Pt 3):715-22. doi: [10.1093/brain/119.3.715](https://doi.org/10.1093/brain/119.3.715). [PubMed: 8673485].
10. Meier DS, Weiner HL, Guttman CR. MR imaging intensity modeling of damage and repair in multiple sclerosis: Relationship of short-term lesion recovery to progression and disability. *AJNR Am J Neuroradiol*. 2007;**28**(10):1956-63. doi: [10.3174/ajnr.A0701](https://doi.org/10.3174/ajnr.A0701). [PubMed: 17998417].
11. Meier DS, Weiner HL, Guttman CR. Time-series modeling of multiple sclerosis disease activity: A promising window on disease progression and repair potential? *Neurotherapeutics*. 2007;**4**(3):485-98. doi: [10.1016/j.nurt.2007.05.008](https://doi.org/10.1016/j.nurt.2007.05.008). [PubMed: 17599713]. [PubMed Central: [PMC7479736](https://pubmed.ncbi.nlm.nih.gov/PMC7479736/)].
12. Nathoo N, Yong VW, Dunn JF. Using magnetic resonance imaging in animal models to guide drug development in multiple sclerosis. *Mult Scler*. 2014;**20**(1):3-11. doi: [10.1177/1352458513512709](https://doi.org/10.1177/1352458513512709). [PubMed: 24263386].
13. Varatharaj A, Liljeroth M, Darekar A, Larsson HBW, Galea I, Cramer SP. Blood-brain barrier permeability measured using dynamic contrast-enhanced magnetic resonance imaging: A validation study. *J Physiol*. 2019;**597**(3):699-709. doi: [10.1113/jp276887](https://doi.org/10.1113/jp276887). [PubMed: 30417928]. [PubMed Central: [PMC6355631](https://pubmed.ncbi.nlm.nih.gov/PMC6355631/)].
14. Hiehle JF, Jr, Grossman RI, Ramer KN, Gonzalez-Scarano F, Cohen JA. Magnetization transfer effects in MR-detected multiple sclerosis lesions: comparison with gadolinium-enhanced spin-echo images and nonenhanced T1-weighted images. *AJNR Am J Neuroradiol*. 1995;**16**(1):69-77. [PubMed: 7900604].
15. Trip SA, Miller DH. Imaging in multiple sclerosis. *J Neurol Neurosurg Psychiatry*. 2005;**76** Suppl 3:iii1-8. doi: [10.1136/jnnp.2005.073213](https://doi.org/10.1136/jnnp.2005.073213). [PubMed: 16107385]. [PubMed Central: [PMC1765701](https://pubmed.ncbi.nlm.nih.gov/PMC1765701/)].
16. Carroll WM. 2017 McDonald MS diagnostic criteria: Evidence-based revisions. *Mult Scler*. 2018;**24**(2):92-5. doi: [10.1177/1352458517751861](https://doi.org/10.1177/1352458517751861). [PubMed: 29451442].
17. Tofts PS, Brix G, Buckley DL, Evelhoch JL, Henderson E, Knopp MV, et al. Estimating kinetic parameters from dynamic contrast-enhanced T1-weighted MRI of a diffusible tracer: Standardized quantities and symbols. *J Magn Reson Imaging*. 1999;**10**(3):223-32. doi: [10.1002/\(sici\)1522-2586\(199909\)10:3<223::aid-jmri2>3.0.co;2-s](https://doi.org/10.1002/(sici)1522-2586(199909)10:3<223::aid-jmri2>3.0.co;2-s). [PubMed: 10508281].
18. Frischer JM, Bramow S, Dal-Bianco A, Lucchinetti CF, Rauschka H, Schmidbauer M, et al. The relation between inflammation and neurodegeneration in multiple sclerosis brains. *Brain*. 2009;**132**(Pt 5):1175-89. doi: [10.1093/brain/awp070](https://doi.org/10.1093/brain/awp070). [PubMed: 19339255]. [PubMed Central: [PMC2677799](https://pubmed.ncbi.nlm.nih.gov/PMC2677799/)].
19. Quarantelli M. MRI/MRS in neuroinflammation: methodology and applications. *Clin Transl Imaging*. 2015;**3**:475-89. doi: [10.1007/s40336-015-0142-y](https://doi.org/10.1007/s40336-015-0142-y). [PubMed: 26705534]. [PubMed Central: [PMC4679099](https://pubmed.ncbi.nlm.nih.gov/PMC4679099/)].
20. Reitz SC, Hof SM, Fleischer V, Brodski A, Groger A, Gracien RM, et al. Multi-parametric quantitative MRI of normal appearing white matter in multiple sclerosis, and the effect of disease activity on T2. *Brain Imaging Behav*. 2017;**11**(3):744-53. doi: [10.1007/s11682-016-9550-5](https://doi.org/10.1007/s11682-016-9550-5). [PubMed: 27138529].

21. Xiong H, Yin P, Li X, Yang C, Zhang D, Huang X, et al. The features of cerebral permeability and perfusion detected by dynamic contrast-enhanced magnetic resonance imaging with Patlak model in relapsing-remitting multiple sclerosis. *Ther Clin Risk Manag.* 2019;**15**:233–40. doi: [10.2147/TCRM.S189598](https://doi.org/10.2147/TCRM.S189598). [PubMed: [30787618](https://pubmed.ncbi.nlm.nih.gov/30787618/)]. [PubMed Central: [PMC6366346](https://pubmed.ncbi.nlm.nih.gov/PMC6366346/)].
22. Popescu BF, Pirko I, Lucchinetti CF. Pathology of multiple sclerosis: Where do we stand? *Continuum (Minneapolis Minn).* 2013;**19**(4 Multiple Sclerosis):901–21. doi: [10.1212/01.CON.0000433291.23091.65](https://doi.org/10.1212/01.CON.0000433291.23091.65). [PubMed: [23917093](https://pubmed.ncbi.nlm.nih.gov/23917093/)]. [PubMed Central: [PMC3915566](https://pubmed.ncbi.nlm.nih.gov/PMC3915566/)].
23. Ingrisch M, Sourbron S, Herberich S, Schneider MJ, Kumpfel T, Hohlfeld R, et al. Dynamic contrast-enhanced magnetic resonance imaging suggests normal perfusion in normal-appearing white matter in multiple sclerosis. *Invest Radiol.* 2017;**52**(3):135–41. doi: [10.1097/RLI.0000000000000320](https://doi.org/10.1097/RLI.0000000000000320). [PubMed: [27548346](https://pubmed.ncbi.nlm.nih.gov/27548346/)].
24. Wen J, Yablonskiy DA, Luo J, Lancia S, Hildebolt C, Cross AH. Detection and quantification of regional cortical gray matter damage in multiple sclerosis utilizing gradient echo MRI. *Neuroimage Clin.* 2015;**9**:164–75. doi: [10.1016/j.nicl.2015.08.003](https://doi.org/10.1016/j.nicl.2015.08.003). [PubMed: [27330979](https://pubmed.ncbi.nlm.nih.gov/27330979/)]. [PubMed Central: [PMC4907986](https://pubmed.ncbi.nlm.nih.gov/PMC4907986/)].
25. Ingrisch M, Sourbron S, Morhard D, Ertl-Wagner B, Kumpfel T, Hohlfeld R, et al. Quantification of perfusion and permeability in multiple sclerosis: Dynamic contrast-enhanced MRI in 3D at 3T. *Invest Radiol.* 2012;**47**(4):252–8. doi: [10.1097/RLI.0b013e31823bfc97](https://doi.org/10.1097/RLI.0b013e31823bfc97). [PubMed: [22373532](https://pubmed.ncbi.nlm.nih.gov/22373532/)].
26. Sahraian MA, Radue EW, Haller S, Kappos L. Black holes in multiple sclerosis: definition, evolution, and clinical correlations. *Acta Neurol Scand.* 2010;**122**(1):1–8. doi: [10.1111/j.1600-0404.2009.01221.x](https://doi.org/10.1111/j.1600-0404.2009.01221.x). [PubMed: [20003089](https://pubmed.ncbi.nlm.nih.gov/20003089/)].
27. Vavasour IM, Laule C, Li DK, Traboulsee AL, MacKay AL. Is the magnetization transfer ratio a marker for myelin in multiple sclerosis? *J Magn Reson Imaging.* 2011;**33**(3):713–8. doi: [10.1002/jmri.22441](https://doi.org/10.1002/jmri.22441). [PubMed: [21563257](https://pubmed.ncbi.nlm.nih.gov/21563257/)].
28. Schmierer K, Scaravilli F, Altmann DR, Barker GJ, Miller DH. Magnetization transfer ratio and myelin in postmortem multiple sclerosis brain. *Ann Neurol.* 2004;**56**(3):407–15. doi: [10.1002/ana.20202](https://doi.org/10.1002/ana.20202). [PubMed: [15349868](https://pubmed.ncbi.nlm.nih.gov/15349868/)].
29. Bot JC, Blezer EL, Kamphorst W, Lycklama AG, Ader HJ, Castelijns JA, et al. The spinal cord in multiple sclerosis: Relationship of high-spatial-resolution quantitative MR imaging findings to histopathologic results. *Radiology.* 2004;**233**(2):531–40. doi: [10.1148/radiol.2332031572](https://doi.org/10.1148/radiol.2332031572). [PubMed: [15385682](https://pubmed.ncbi.nlm.nih.gov/15385682/)].
30. Ge Y. Multiple sclerosis: the role of MR imaging. *AJNR Am J Neuroradiol.* 2006;**27**(6):1165–76. [PubMed: [16775258](https://pubmed.ncbi.nlm.nih.gov/16775258/)].
31. Fooladi M, Riahi Alam N, Harirchyan MH, Firuznia K, Oghabian MA, Shakiba M, et al. The assessment of structural changes in ms plaques and normal appearing white matter using quantitative magnetization transfer imaging (MTI). *Iran J Med Physics.* 2007;**4**(3, 4):53–64.
32. Liu Z, Pardini M, Yaldizli O, Sethi V, Muhlert N, Wheeler-Kingshott CA, et al. Magnetization transfer ratio measures in normal-appearing white matter show periventricular gradient abnormalities in multiple sclerosis. *Brain.* 2015;**138**(Pt 5):1239–46. doi: [10.1093/brain/awv065](https://doi.org/10.1093/brain/awv065). [PubMed: [25823475](https://pubmed.ncbi.nlm.nih.gov/25823475/)]. [PubMed Central: [PMC5963416](https://pubmed.ncbi.nlm.nih.gov/PMC5963416/)].